Combination of *Sophora flavescens* alkaloids and Panax quinquefolium saponins modulates different stages of experimental autoimmune myocarditis via the NF-κB and TGF-β1 pathways

MENGHUI LIU[1,2*], YUE LIN[1,3*], HUIBO XU[3], LIXIN LI[2] and TAO DING[3]

[1]Department of Traditional Chinese Medicine, Changchun University of Traditional Chinese Medicine; [2]Department of Pediatrics, and [3]Pharmacodynamic and Toxicological Evaluation Center, Jilin Academy of Traditional Chinese Medicine, Changchun, Jilin 130000, P.R. China

Received March 31, 2022; Accepted June 29, 2022

DOI: 10.3892/etm.2022.11507

Abstract. Chronic cardiac inflammation and fibrosis can progress into severe forms of cardiomyopathy. *Sophora flavescens* alkaloids (KuShen) have been previously reported to exert anti-inflammatory effects, whereas *Panax quinquefolium* saponins (XiYangShen) has been shown to alleviate cardiac fibrosis. Therefore, the potential effects of their combination (KX) on different stages of autoimmune myocarditis were investigated in the present study. Mice were randomly divided into the following four groups: Control; experimental autoimmune myocarditis (EAM); KX-High (275 mg/kg); and KX-Low (138 mg/kg). A 21-day and a 60-day EAM model was established through multi-site subcutaneous injections of cardiac myosin mixed with complete Freund's adjuvant on days 0, 7, 21 and 42. Mice in the High and Low KX groups were treated by gavage (10 ml/kg) daily from day 0 (1 day before treatment) until sacrifice (day 21 or 60). Mice in the control and EAM groups received an equivalent volume of distilled water. The levels of lactate dehydrogenase (LDH), creatine kinase-myocardial band (CK-MB), cardiac troponin I (cTn-I), IL-1β, IL-6, TNF-α, TGF-β1, collagen type I (Col I) and collagen type III (Col III) were measured by ELISA in the mouse myocardial tissues or serum. Myocardial tissue structure and extent of fibrosis were visualized using H&E and Masson's staining. Western blotting and immunohistochemistry were used to measure the expression levels NF-κB and TGF-β1 pathway proteins in the myocardial tissues. The degree of inflammation in the 21-day EAM model was found to be significantly higher compared with that in the 60-day EAM model. KX significantly reduced the inflammatory response at 21 days by decreasing the expression levels of CK-MB, LDH, cTn-I, IL-1β, IL-6, TNF-α and TGF-β-activated kinase 1-binding protein 1/NF-κB pathway proteins. Myocardial fibrosis in the 60-day EAM model was also significantly worse compared with that in the 21-day EAM model. However, fibrosis was significantly delayed by treatment with KX. In addition, KX significantly decreased the expression levels of TGF-β1, Smad2, Smad4, Col I and Col III. Therefore, these data suggest that KX is beneficial for treating myocarditis by targeting multiple pathways.

Correspondence to: Dr Lixin Li, Department of Pediatrics, Jilin Academy of Traditional Chinese Medicine, 1705 Gongnong Road, Changchun, Jilin 130000, P.R. China
E-mail: 1487677244@qq.com

Dr Tao Ding, Pharmacodynamic and Toxicological Evaluation Center, Jilin Academy of Traditional Chinese Medicine, 155 Chuangju Street, Changchun, Jilin 130000, P.R. China
E-mail: 202002705048@stu.ccucm.edu.cn

*Contributed equally

Abbreviations: KX, combination of *Sophora flavescens* alkaloids (KuShen) and *Panax quinquefolium saponins* (XiYangShen); EAM, experimental autoimmune myocarditis; TCM, traditional Chinese medicine

Key words: Sophora flavescens alkaloids, *Panax quinquefolium* saponins, KX, autoimmune myocarditis, inflammation, myocardial fibrosis

Introduction

Myocarditis is cardiac inflammation that can be caused by viruses, bacteria or autoimmune diseases (1). The development of myocarditis can be divided into two stages. The first stage involves humoral immunity and pathogen-mediated cellular immune activation, inflammatory cytokine production and pathway activation, leading to apparent cardiomyocyte necrosis. The second stage is characterized by chronic inflammation of the myocardium, which causes myocardial remodeling and fibrosis, ultimately progressing into dilated cardiomyopathy (DCM) (2). Autoimmunity one of the main pathological causes of the development of myocarditis. Myocardial inflammatory injury promotes myocardial fibrosis, which is critical to the progression of myocarditis into DCM (3,4). Since the different stages of myocarditis exhibit different pathological characteristics, distinct therapeutic approaches may be

required. Inhibiting the inflammatory response during the first stage of myocarditis and myocardial fibrosis during the second stage may serve important implications for disease outcomes (2). Experimental autoimmune myocarditis (EAM) mouse models have immunological features paralleling and resembling the myocarditis in humans, making it suitable for pursuing pathophysiological insights into myocarditis (5). In this model, autoimmune myocarditis can be induced by the subcutaneous inoculation of susceptible mice with cardiac myosin and complete Freund's adjuvant (6). The first 21 days after inoculation can be considered to correspond to the first stage of myocarditis in humans (6,7). At this stage, antibody deposition in cardiomyocytes leads to apoptosis, which in turn activates cellular and humoral immunity. A large number of natural killer, T and other immune cell types can infiltrate the myocardial tissue (7). This process leads to the release of large quantities of IL-1β, TNF, IL-6 and other inflammatory cytokines, exacerbating myocardial injury (7-11). Subsequently, the inflammation would normally begin to subside, whilst the secretion of TGF-β and collagen in the myocardium is also increased (12). This is a characteristic of the progressive accumulation of fibrotic tissues in the myocardium, which dilates the ventricles and impair cardiac function (12), in a manner that is equivalent to the second stage of myocarditis. This EAM mouse model is frequently used to study the different stages of myocarditis pathogenesis (13). Intervention at different stages of myocarditis development in animal models would be beneficial for studying the effects of potential therapeutic agents at different time points of administration.

Supportive therapies and immunosuppression remain to be the main treatment methods for myocarditis (1). However, side effects, such as weight gain, reduced immunity and hypertension, often occur after treatment (14-16). Therefore, it is important to identify novel therapeutic agents that may be beneficial for patients with myocarditis. According to the theory of traditional Chinese medicine (TCM), radix *Sophora* may treat inflammatory cardiomyopathy, while *Panax quinquefolium* is effective in Dilated cardiomyopathy (17). Pharmacological studies involving rheumatoid arthritis models have previously shown that *Sophora flavescens* alkaloids can inhibit NF-κB signaling and reduce the levels of TNF-α and IL-6 (18). By contrast, *Panax quinquefolium* saponins have been shown to serve a protective role in cardiac injury by attenuating cardiac fibrosis and remodeling in rats with heart failure through the TGF-β1/Smad pathway (19,20). In addition, *Panax quinquefolium* saponins were found to ameliorate cardiac remodeling and myocardial fibrosis in rat models of chronic thromboembolic pulmonary hypertension (17,21). However, to the best of our knowledge, all previous studies mainly assessed the efficacy of single drugs or compounds at a certain stage of myocarditis. Therefore, the previous findings aforementioned may not completely reflect the therapeutic characteristics and advantages of combined treatment with TCM (22,23).

Alkaloids and saponins are the main pharmacologically active components of *Sophora flavescens* and *Panax quinquefolium*, respectively (24,25). In the present study, an autoimmune myocarditis animal model was used to observe the effects of *Sophora flavescens* alkaloids (KuShen) and *Panax quinquefolium* saponins [XiYangShen; combination of KuShen and XiYangShen (KX)] at different stages of myocarditis. The mechanisms of action of KX were also explored to provide an experimental basis for the future clinical application of this formulation. To the best of our knowledge, the present study is the first to investigate the effects of KX on different stages of autoimmune myocarditis.

Materials and methods

Animals. A total of 96 male BALB/c mice aged 6-8 weeks (weight, 18-20 g) were purchased from Changchun Changsheng Gene Pharmaceutical Co., Ltd. [license number: SCXK (Liao)-2020-0001; eligibility nos. 2107262101007676 and 21072621030386012]. Mice were housed in a barrier system at a temperature of 23±2˚C, humidity of 60±10% and a 12/12-h light/dark cycle. All animals had free access to food and water. The present study was approved by the animal Ethics Committee of the Jilin Academy of TCM (approval no. JLSZ KYDWLL2021-003; Changchun, China).

Composition, ratio and concentration selection of KX. The *Sophora flavescens* alkaloids were composed by mixing matrine ($C_{15}H_{24}N_2O$) and oxymatrine ($C_{15}H_{24}N_2O_2$) in a 1:1 ratio. The purity of the *Panax quinquefolium* saponins, consisting of ginsenoside Rg1 ($C_{42}H_{72}O_{14}$), ginsenoside Re ($C_{48}H_{82}O_{18}$) and ginsenoside rb1 ($C_{54}H_{92}O_{23}$), was determined to be ≥70% through high-performance liquid chromatography. All these compounds were provided by the New Drug Center of the Jilin Academy of TCM.

Optimization of the compound formula was performed using the uniform design model (a mathematical method) to reduce the experiment times, the uniform design and data analysis were performed using DPS v. 6.55 software. (26). Subsequently, EAM rat model was used to determine the optimal group ratio of *Sophora flavescens* alkaloids to *Panax quinquefolium* saponins, which was 1.1:1. At that ratio, it significantly alleviated myocardial injury (27).

EAM induction and KX treatment. After 1 week of adaptive feeding, BALB/c mice were randomly divided into the following groups based on body weight (24 animals per group): Control; EAM; KX-High (KX dose, 275 mg/kg); and KX-Low (KX dose, 138 mg/kg). All mice, except for those in the control group, received subcutaneous (back, inguinal on both sides) injections of 0.2 ml emulsion I on days 0, 7, 21 and 42 at the beginning of the test. Porcine cardiac myosin (MilliporeSigma) was dissolved in potassium phosphate buffer (pH=6.8) and mixed thoroughly 1:1 with complete Freund's adjuvant (MilliporeSigma), yielding a solution with 200 μg porcine cardiac myosin in 0.2 ml of the emulsion (6).

In the control group, each animal was injected with 0.2 ml emulsion II (potassium phosphate buffer with complete Freund's adjuvant at a 1:1 ratio) following the same protocol. High and Low KX solutions were prepared by dissolving 275 or 138 mg KX, respectively, in 10 ml distilled water. Mice in the KX-high and KX-low groups were intragastrically fed by oral gavage (10 ml/kg) with the experimental drug daily from day 0 until sacrifice (day 21 or 60). Mice in the control and EAM groups received an equivalent volume of distilled water. All animals were anesthetized by an intraperitoneal injection of sodium

pentobarbital (50 mg/kg) and then euthanized through cervical dislocation. In addition, mice were anesthetized and sacrificed before the experimental endpoints in case of persistent self-injurious behavior, non-healing wounds and loss of appetite.

Histopathology. Mice were sacrificed after 21 or 60 days, before their bodyweight and heart weight were measured. The heart tissues were fixed in 15% formalin at a temperature of 23±2˚C for not less than 48 h, embedded in paraffin and sectioned into transverse sections (5-μm thickness) for H&E staining (at a temperature of 23±2˚C for 5-20 min). For the H&E staining, myocardial tissue was examined under a light microscope at a magnification of x400, the macroscopic score was determined using a five-point scale: 0, no inflammation; 1, limited discoloration; 2, numerous small lesions; 3, diffused discoloration not exceeding one-third of the heart surface; and 4, diffused discoloration exceeding one-third of the heart surface (28). After processing the myocardial tissues in the same manner, Masson's trichrome staining (at a temperature of 23±2˚C for 5-10 min) was also performed. Myocardial tissue was examined under a light microscope at a magnification of x400 and scored using ImageJ (version 1.5.1; National Institutes of Health).

Immunohistochemical analysis. After deparaffinization (the tissue sections were immersed in xylene for 10 min and re-soaked in xylene for another 10 min at a temperature of 23±2˚C) and rehydration (descending ethanol hydration 100, 95, 90 and 80%) of the paraffin sections, tissues sections were immersed in citrate buffer (pH 6.0; Wuhan Boster Biological Technology, Ltd.; cat. no. AR0024) for 15 min at room temperature for antigen retrieval. All sections were incubated in H_2O_2 (3%)to block endogenous peroxidase activity. This step was followed by incubation in 5%BSA (Wuhan Boster Biological Technology, Ltd.; cat. no. AR0004) for 10 min at room temperature to block nonspecific antigen-binding sites. Subsequently, the sections were incubated with primary antibodies (Santa Cruz Biotechnology, Inc.) against NF-κB (cat. no. sc-8008; 1:200 dilution) and TGF-β1 (cat. no. sc-130348; 1:200 dilution) overnight at 4˚C, followed by incubation with HRP-conjugated secondary antibodies (ProteinTech Group, Inc; cat. no. SA00001-2; 1:2,000 dilution) for 60 min at 4˚C. Then, sections were counter-stained with DAB and hematoxylin for 3-10 min to distinguish between cytoplasm and nucleus at room temperature. After dehydration in ddH2O at room temperature, 90% ethanol for 5 min, 95% ethanol for 5 min, twice in 100% ethanol for 5 min and n-butanol for 5 min, and permeabilization in xylene for 5 min, sections were mounted using neutral gum. Positive staining was observed under a light microscope (Olympus BX51; Olympus Corporation). A total of five fields of view were randomly selected for each tissue section and observed at a magnification of x100.

ELISA analysis. The serum levels of CK-myocardial band (CK-MB), LDH and the cardiac tissue levels of cardiac troponin I (cTn-I), collagen type I (Col I), collagen type III (Col III) and the inflammatory markers IL-1β, IL-6, TNF-α and TGF-β1 were detected using mouse ELISA kits (R&D Systems China Co., Ltd.: CK-MB, cat. no. 202109; LDH, cat. no. 202108; cTn-I, cat. no. 202108; Col I, cat. no. 202110; IL-1β, cat. no. 202109; IL-6, cat. no. 202108; TNF-α cat. no. 202107 and TGF-β1 cat. no. 202109). Cardiac homogenate (10%) was prepared by grinding 100 mg of heart tissue in 1 ml of saline. In microplates, standards (50 μl) were added into predefined wells, samples (10 μl serum or cardiac homogenate) and sample diluent (40 μl) were added into testing sample wells, while blank wells were left empty. In the wells for standards and samples, horseradish peroxidase-labelled conjugates (100 μl) were added before sealing the plates for incubation at 37˚C for 60 min. After washing the plates 5 times, substrates A (50 μl) and B (50 μl) were added into each well. After incubation at 37˚C for 15 min, stop solution (50 μl) was added to each well, and the absorbance of each well was measured at 450 nm within 15 min (cat. no. ELx800; BioTek Instruments, Inc.).

Western blotting. Protein extracts from cardiac tissue were prepared in Radio-Immunoprecipitation Assay (RIPA) lysis buffer (CoWin Biosciences; cat. no. 21821) containing protease and phosphatase inhibitors. Proteins were separated through 10% SDS-PAGE and transferred onto nitrocellulose membranes. After blocking in 5% non-fat milk diluted in TBS-Tween 20 (0.1% Tween; CoWin Biosciences) in the dark at 4˚C overnight, the membranes were incubated with primary antibodies (Santa Cruz Biotechnology, Inc.) against activated kinase 1 (TAK1)-binding protein 1 (TAB1, cat. no. sc-166138; 1:100 dilution), NF-κB (cat. no. sc-8008; 1:200 dilution), phosphorylated (p)-NF-κB (cat. no. sc-136548; 1:200 dilution), IκB (cat. no. sc-74451; 1:100 dilution), p-IκB (cat. no. sc-8404; 1:200 dilution), IKKα (cat. no. sc-7606; 1:200 dilution), TGF-β1 (cat. no. sc-130348; 1:200 dilution), Smad2 (cat. no. sc-101153; 1:200 dilution), Smad4(cat. no. sc-7966; 1:200 dilution), Col I (cat. no. sc-376350; 1:100 dilution) or GAPDH (cat. no. sc-365062; 1:100 dilution) for 2 h at 37˚C. Subsequently, the membranes were washed by TBS-Tween-20 and incubated with a secondary HRP-conjugated antibody (m-IgGκ, cat. no. sc-516102; 1:1,000 dilution or m-IgG Fc, cat. no. sc-525409; 1:1,000 dilution; Santa Cruz Biotechnology, Inc.) for 1.5 h at 37˚C. Next, the incubated membranes were washed again and visualized using an enhanced chemiluminescence detection kit (CoWin Biosciences). The levels of target proteins were normalized to those of GAPDH with Gel imaging system (ChemiDoc-It 510 Imager, Ultra-Violet Products Ltd).

Statistical analysis. GraphPad Prism software (version 9.0; GraphPad Software Inc.) was used for all statistical analyses. Statistical analysis was performed using two-way analysis of variance (ANOVA) with Bonferroni post hoc tests for comparisons between different time points and groups and one-way ANOVA with Tukey's post hoc test or Kruskal-Wallis followed by Dunn's post hoc test for the comparison among multiple groups. The macroscopic scores are presented as the median + interquartile range, whilst all other values are presented as the mean ± standard deviation. $P<0.05$ was considered to indicate a statistically significant difference.

Results

Effects of KX on the cardiac indices of mice. After 21 days, mice in the EAM group weighed significantly less compared with those in the control group ($P<0.01$; Fig. 1A), whilst

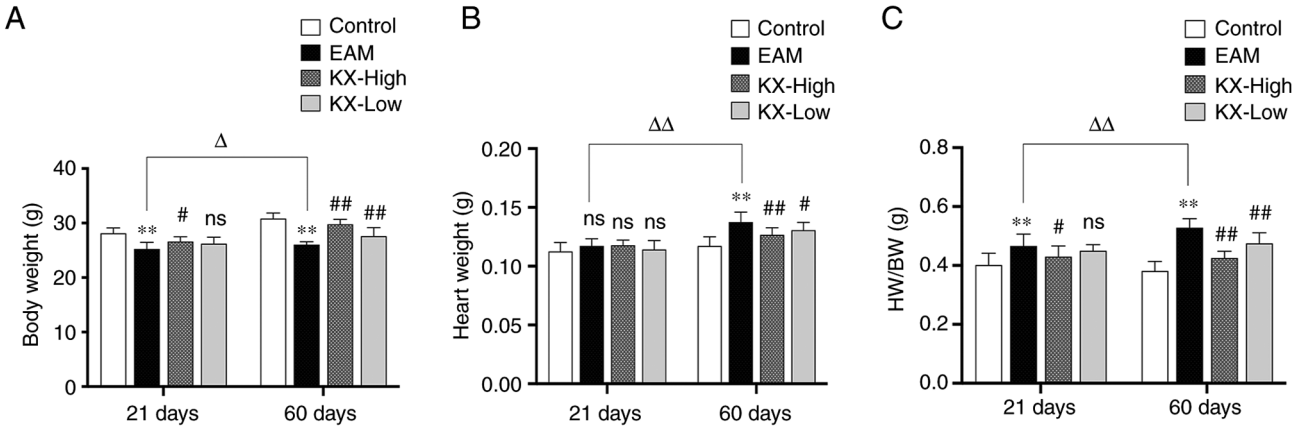

Figure 1. Effects of KX on the mouse cardiac indices after 21 and 60 days. (A) Body weight (n=12 per group). (B) Changes in heart weight (n=12 per group). (C) Changes in HW/BW (n=12 per group). **P<0.01 vs. Control; $^{\#}$P<0.05 and $^{\#\#}$P<0.01 vs. EAM. $^{\Delta}$P<0.05 and $^{\Delta\Delta}$P<0.01. EAM, experimental autoimmune myocarditis; KX, combination of *Sophora flavescens* alkaloids (KuShen) and *Panax quinquefolium saponins* (XiYangShen); ns, not significant; HW, heart weight; BW, body weight.

those in the KX-high group gained weight significantly more efficiently compared with those in the EAM group (P<0.05; Fig. 1A). However, no significant changes in heart weight was observed (P>0.05; Fig. 1B). The HW/BW was significantly higher in the EAM group compared with that in the control group (P<0.01; Fig. 1C), whereas it was significantly decreased in the KX-high group compared with that in the EAM group (P<0.05; Fig. 1C). However, there were no significant changes in KX-low group (P>0.05; Fig. 1C).

After 60 days, the mice in the EAM group weighed significantly less compared with those in the control group (P<0.01; Fig. 1A), whilst those in the KX group were significantly heavier compared with those recorded in the EAM group (P≤0.05; Fig. 1A). The heart weight was significantly higher in the EAM group compared with that in the control group, which was reduced following intervention with KX (P<0.01; Fig. 1B). The HW/BW was also significantly higher in the EAM group compared with that in the control group, which was in turn significantly reduced following intervention with KX (P<0.01; Fig. 1C).

In the control group, no changes were observed in the body weight of mice sacrificed after 21 and 60 days. In the EAM group, the HW/BW was significantly increased (P<0.01; Fig. 1) after 60 days compared with that after 21 days.

Effects of KX on myocardial injury in mice. After 21 days, the serum levels of CK-MB, LDH and cTn-I were significantly increased in the EAM group compared with those in the control group (P<0.01; Fig. 2A-C). Compared with those in the EAM group, the aforementioned indices were significantly decreased after treatment with KX (P<0.01; Fig. 2A-C).

After 60 days, the serum levels of CK-MB, LDH and cTn-I were significantly increased in the EAM group compared with those in the control group (P<0.01; Fig. 2A-C). Compared with those in the EAM group, the aforementioned indices were significantly decreased in the KX-high group (P<0.01 or P<0.05), but in a dose-dependent manner relationship (Fig. 2A-C). H&E staining of the myocardial tissues showed that, compared with that in the control group, the EAM group exhibited inflammatory cell infiltration and myocardial tissue damage after both 21 and 60 days (P<0.01). However, this inflammatory damage was significantly alleviated following treatment with high-dose KX (Fig. 2D; P<0.05).

In control mice, there were no changes observed between 21 and 60 days. However, the levels of CK-MB, LDH and cTn-I were significantly lower after 60 days compared with those after 21 days (P<0.01; Fig. 2A-C).

Effects of KX on inflammatory factors in the mouse myocardium. After 21 days, the levels of IL-6, IL-1β and TNF-α were significantly increased in the EAM group compared with those in the control group (P<0.01; Fig. 3A-C). Compared with those in the EAM group, these levels were significantly reduced after intervention with KX (P<0.01; Fig. 3A-C).

After 60 days, the levels of IL-6, IL-1β and TNF-α were significantly higher in the EAM group compared with those in the control group (P<0.01; Fig. 3A-C). Compared with those in the EAM group, these levels were significantly lower after treatment with high-dose KX (P<0.01 or P<0.05; Fig. 3A-C), but in a dose-dependent manner.

There were no changes observed in terms of the inflammatory cytokines measured in the present study in the control mice between 21 and 60 days. However, in the EAM group the levels of IL-6, IL-1β and TNF-α were significantly lower in the myocardium of mice after 60 days compared with those in mice after 21 days (P<0.01; Fig. 3).

Effects of KX on TAB1 and NF-κB signaling in the mouse myocardium. After 21 days, the expression levels of TAB1, IKKα, p-IκB/IκB, p-NF-κB/NF-κB and TGF-β1 were significantly increased in EAM mice compared with those in the control group (P<0.01; Fig. 4A and B). These levels were significantly decreased (P<0.01 or P<0.05; Fig. 4A and B) after intervention with KX. TAB1 appeared as two bands, which may be a consequence of the expression of the TAB isoforms (Fig. 4A).

The expression of NF-κB and TGF-β1 in the myocardium was next examined using immunohistochemistry. The results showed that their levels were significantly increased (P<0.01)

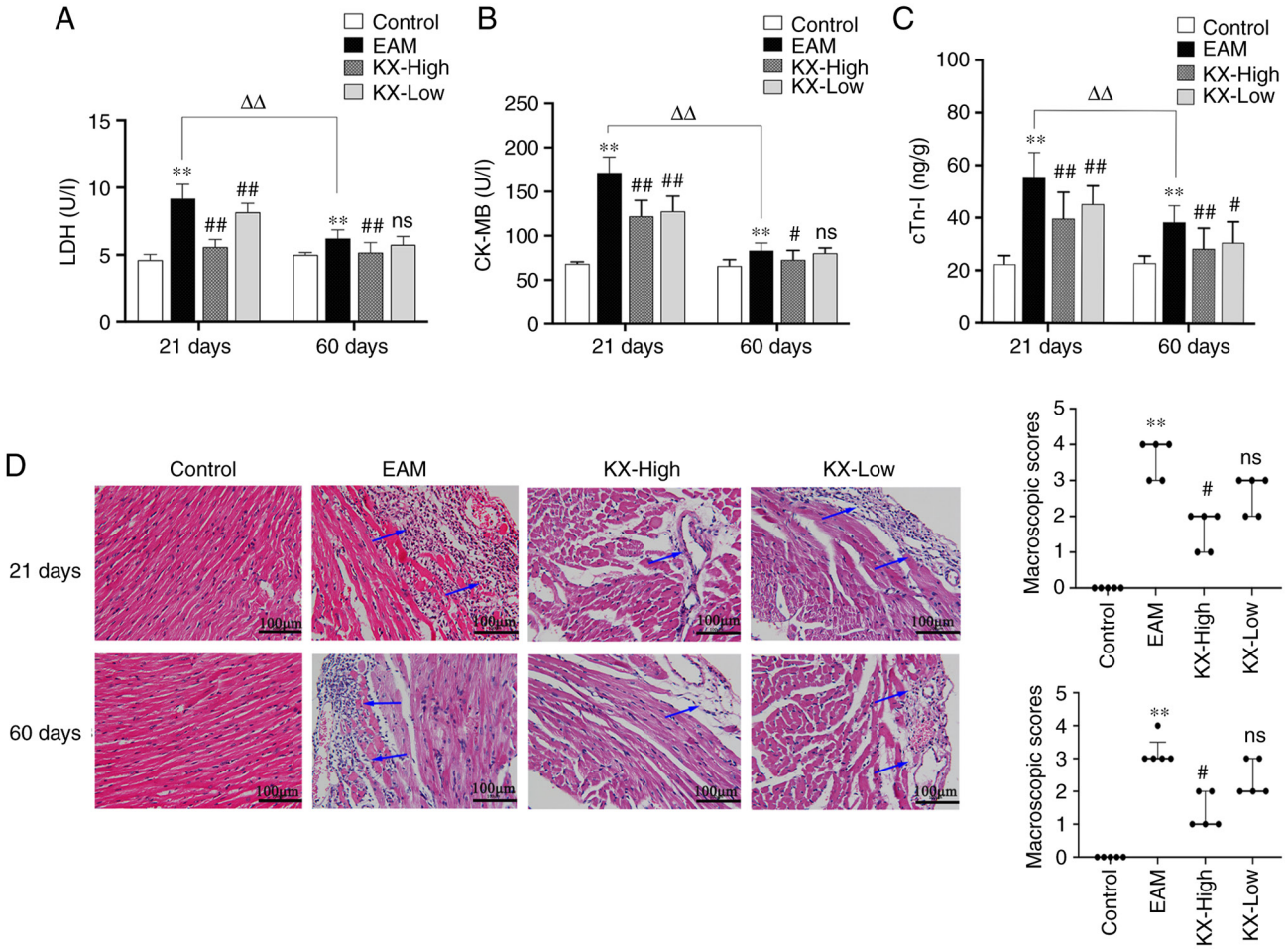

Figure 2. Effects of KX on myocardial injury in mice after 21 and 60 days. Changes in the levels of (A) LDH and (B) CK-MB in mouse serum. (C) Changes in the levels of cTn-I in the myocardium. (D) H&E staining of the myocardium. Scale bars, 100 μm. n=5 per group. Arrows indicate inflammatory cell infiltration (mainly lymphocytes) and myocardial injury. Quantified data plots are shown on the right. **P<0.01 vs. Control; $^{\#}$P<0.05, $^{\#\#}$P<0.01 vs. EAM. $^{\Delta\Delta}$P<0.01. KX, combination of *Sophora flavescens* alkaloids (KuShen) and *Panax quinquefolium saponins* (XiYangShen); LDH, lactate dehydrogenase; CK-MB, creatine kinase-myocardial band; cTn-I, cardiac troponin I; EAM, experimental autoimmune myocarditis; ns, not significant.

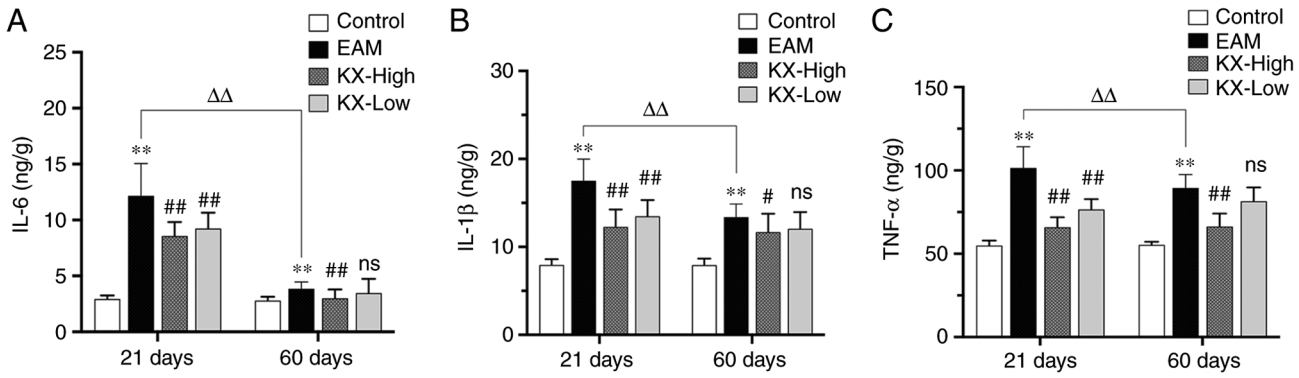

Figure 3. Effects of KX on the production of inflammatory cytokines in the mouse myocardium. Changes in the levels of (A) IL-6, (B) IL-1β and (C) TNF-α in the mouse myocardium (n=12 per group). **P<0.01 vs. Control; $^{\#}$P<0.05 and $^{\#\#}$P<0.01 vs. EAM. $^{\Delta\Delta}$P<0.01. KX, combination of *Sophora flavescens* alkaloids (KuShen) and *Panax quinquefolium saponins* (XiYangShen); EAM, experimental autoimmune myocarditis; ns, not significant.

in the EAM group compared with those in the control group. However, these were significantly reversed (P<0.01 or P<0.05) after intervention with KX (Fig. 4C and D).

Effects of KX on cardiac fibrosis in mice. After 21 days, the levels of TGF-β1 were significantly higher in the myocardium of mice in the EAM group compared with those in the control group (P<0.01). By contrast, the levels of TGF-β1 was significantly lower in the KX-high group compared with those in the EAM group, in a dose-dependent manner (Fig. 5A). However, no significant change was observed in the levels of Col I and Col III (Fig. 5B and C).

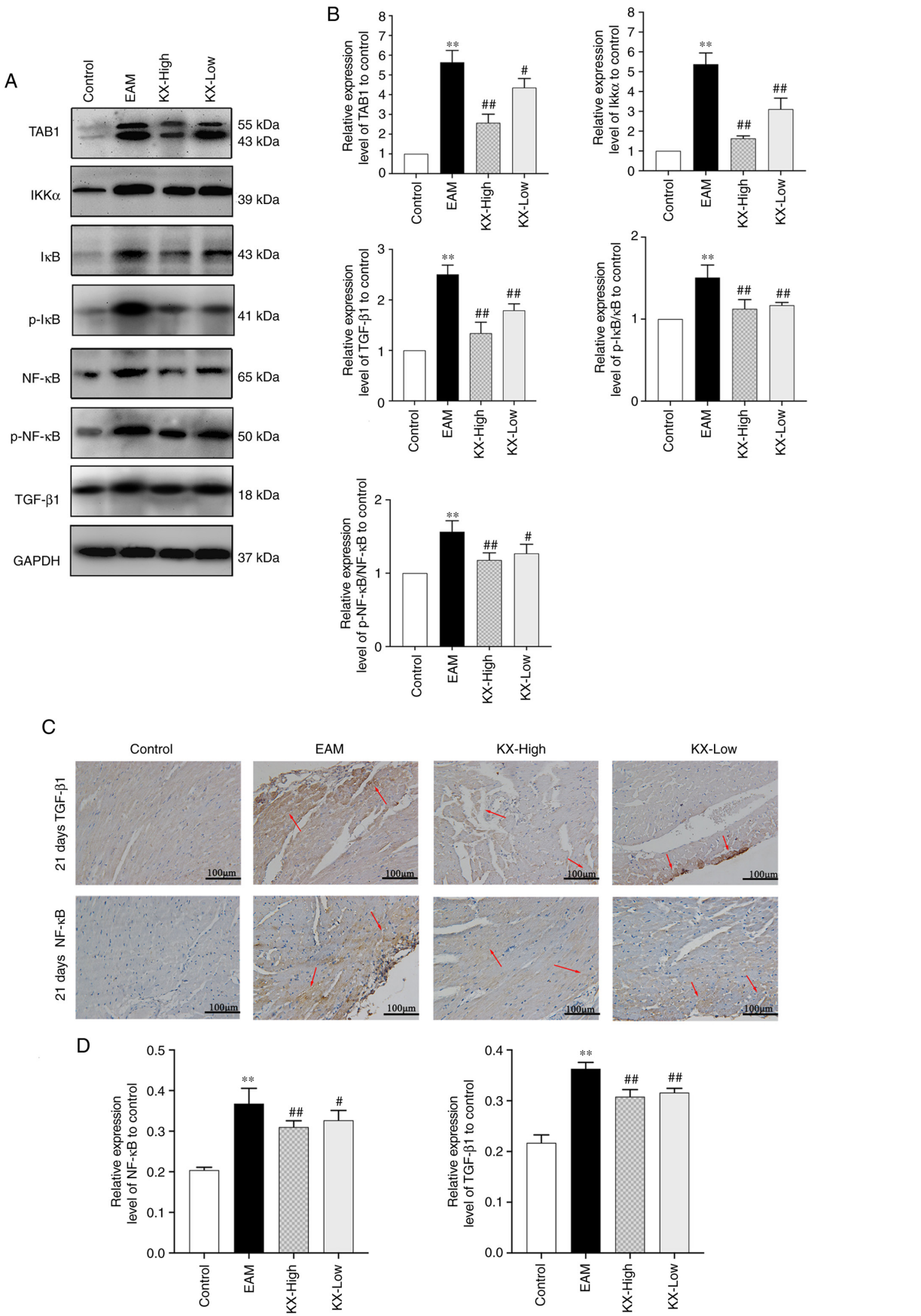

Figure 4. Effects of KX on TAB1 and NF-κB signaling in the mouse myocardium. (A) Western blot analysis of TAB1, IKKα, IκB, p-IκB, NF-κB, p-NF-κB and TGF-β1 protein expression in EAM mice after 21 days. (B) Western blot quantification analysis (n=4 per group). (C) Immunohistochemistry analysis of NF-κB and TGF-β1 expression in EAM mice after 21 days. Scale bar, 100 μm. Arrows indicate positive expression of NF-κB or TGF-β1. (D) Immunohistochemical quantification of NF-κB and TGF-β1 expression in EAM mice after 21 days. n=10 per group. **P<0.01 vs. Control. $^{\#}$P<0.05 and $^{\#\#}$P<0.01 vs. EAM. TAB1, TGF-β activated kinase 1-binding protein 1; EAM, experimental autoimmune myocarditis; KX, combination of *Sophora flavescens* alkaloids (KuShen) and *Panax quinquefolium saponins* (XiYangShen).

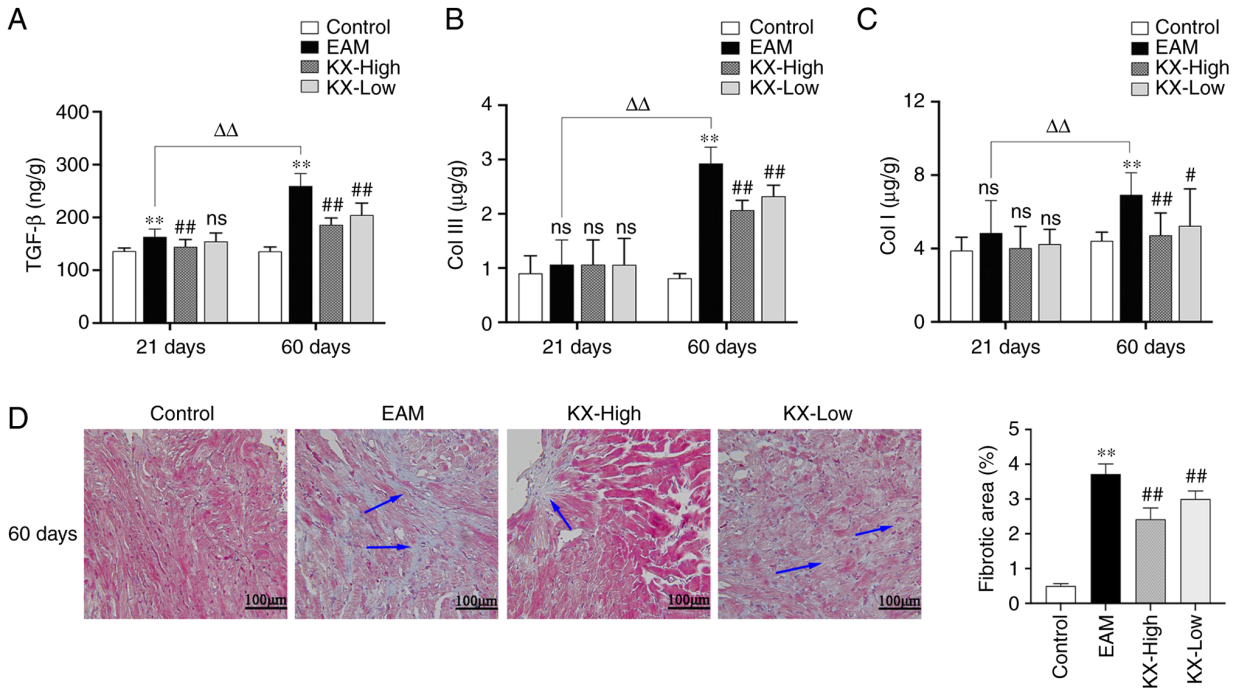

Figure 5. Effects of KX on cardiac fibrosis in mice. Levels of (A) TGF-β1, (B) Col III and (C) Col I after 21 and 60 days (n=12 per group). (D) Masson's trichrome staining of EAM mice after 60 days and corresponding quantification. Scale bar, 100 μm. n=5 per group. Arrows indicate the cardiac muscle fiber. **P<0.01 vs. Control; $^{\#}$P<0.05 and $^{\#\#}$P<0.01 vs. EAM. $^{\Delta\Delta}$P<0.01. EAM, experimental autoimmune myocarditis; KX, combination of *Sophora flavescens* alkaloids (KuShen) and *Panax quinquefolium saponins* (XiYangShen); ns, not significant; Col I, collagen type I; Col III, collagen type III.

After 60 days, the levels of TGF-β1, Col I and Col III were significantly increased in the myocardium of mice in the EAM group compared with those in the control group (P<0.01). Compared with those in the EAM group, these levels were significantly lower in mice after intervention with KX (P<0.01 or P<0.05; Fig. 5A-C). The results of cardiac Masson's Trichrome staining revealed that myocardial fibrosis was significantly worse in EAM mice compared with that in the control group (P<0.01). Compared with that in the EAM group, myocardial fibrosis was significantly ameliorated after intervention with KX (P<0.01; Fig. 5D). In the EAM group, the levels of TGF-β1, Col I and Col III were significantly increased in the myocardium of mice after 60 days compared with those after 21 days (P<0.01; Fig. 5A-C).

Effects of KX on TGF-β1 and Smad2 expression in the mouse myocardium. After 60 days, the levels of TGF-β1, Smad2, Smad4, Col I and NF-κB in the myocardium were significantly increased in EAM mice compared with those in the control group (P<0.01). These increases were significantly reversed in mice after treatment with KX (P<0.01 or P<0.05; Fig. 6A and B).

NF-κB and TGF-β1 expression in mouse myocardium was subsequently assessed using immunohistochemistry. These results showed that the expression of NF-κB and TGF-β1 was significantly increased in EAM mice compared with that in the control group (P<0.01), which was in turn significantly reversed after treatment with KX (P<0.01; Fig. 6C and D).

Discussion

Myocarditis can manifest with a variety of symptoms, such as palpitations, chest pain and arrhythmia (29). Based on the dialectical treatments described in TCM, Radix *Sophorae flavescentis* and *Panax quinquefolium* can be combined to treat myocarditis, thereby providing the superior synergistic effects of these Chinese herbs (30). In our unpublished studies, *in vitro* tissue culture and *in vivo* viral myocarditis animal models were used to perform antiviral pharmacodynamic experiments using different concentrations of KX. The results of these studies showed that at 0.781 and 0.391 g/l, KX was efficient against HeLa cell cytopathy induced by various enteroviruses, such as coxsackievirus B3 (CVB3), CVB4, CVA16 and enterovirus E71. In addition, the results of these studies showed that at 275 and 138 mg/kg, KX exerted significant therapeutic effects on BALB/c mice with viral myocarditis by reducing aspartate aminotransferase, creatine kinase (CK) and lactate dehydrogenase (LDH) levels in serum. Based on results from a previous study (27), the main active components of *Sophora flavescens* and *Panax quinquefolium*, namely *Sophora flavescens* alkaloids and *Panax quinquefolium* saponins, respectively, were extracted and applied in EAM mouse models. The purpose of this approach was to identify the effective components of these compounds and control their quality and quantity.

An animal model of EAM was previously produced through the injection of cardiac myosin into susceptible rodents, which lack the immune tolerance mechanisms, to recreate the inflammatory and fibrotic stages of myocarditis (31). Inflammation and fibrosis of the myocardium are two important etiological causes of myocarditis (32). Following an autoimmune attack, a large number of immune cells infiltrate the myocardium, leading to myocardial damage, myocardial structural disintegration and the production of proinflammatory cytokines, such as IL-6, IL-1β and TNF-α (33). This process further exacerbates myocardial damage. After ~21 days, myocarditis

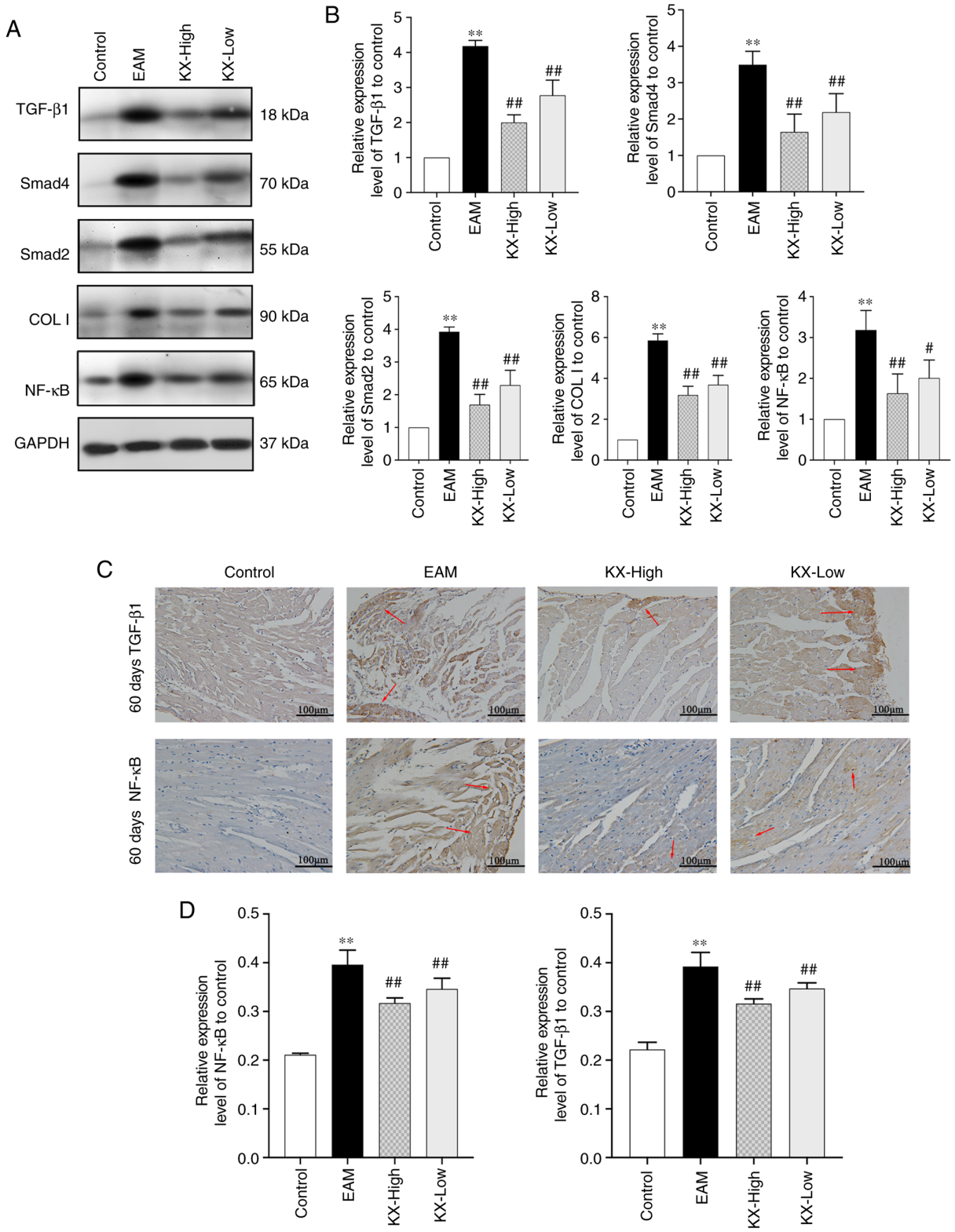

Figure 6. Effects of KX on TGF-β1 and Smad2 expression in the mouse myocardium. (A) TGF-β1, Smad2, Smad4, Col I and NF-κB expression in EAM mice after 60 days. (B) Western blot quantification analysis (n=4 per group). (C) NF-κB and TGF-β1 expression in EAM mice after 60 days. Scale bar, 100 μm. Arrows indicate positive expression of NF-κB or TGF-β1. (D) Quantitative results of immunohistochemical analysis (n=10 per group). **P<0.01 vs. Control; $^{\#}$P<0.05 and $^{\#\#}$P<0.01 vs. the EAM. EAM, experimental autoimmune myocarditis; KX, combination of *Sophora flavescens* alkaloids (KuShen) and *Panax quinquefolium saponins* (XiYangShen); Col I, collagen type I.

advances into the fibrotic stage, where the levels of proinflammatory cytokines decrease but those of profibrotic factors (such as TGF-β1) increase (34). These changes interfere with the regulation of the extracellular matrix architecture and promote the development of fibrosis, thereby replacing necrotic myocardial tissues with collagen protein (35).

In the present study, histopathological analysis of the myocardium revealed marked inflammatory cell infiltration

and the presence of edematous and necrotic tissues in EAM mice sacrificed after 21 days. These observations may be attributed to the activation of the TAB1/NF-κB pathway and the promotion of inflammatory factor expression (IL-6, IL-1β and TNF-α). There were no changes observed in the control group between 21 and 60 days. However, the EAM mice showed reduced inflammatory cell infiltration after 60 days. In addition, increased myocardial tissue damage and fibrosis was observed after 60 days compared with those after 21 days. This may be due to reduced secretion of inflammatory factors in the myocardium, increased activation of the TGF-β1/Smad2 pathway and an increase in the expression of the profibrotic factors TGF-β1, Col I and Col III. These findings suggest that damage may have changed from excessive inflammation at 21 days to myocardial fibrotic damage at 60 days. These are consistent with the results reported in previous studies (36,37).

TNF-α is mainly secreted by mononuclear macrophages and is an important inflammatory and immunomodulatory factor. It is responsible for the immunopathological damage of myocardial cells (38). By contrast, IL-6 is mainly secreted by macrophages and dendritic cells, which contributes to host defenses against infection and tissue injury (39). However, excessive IL-6 synthesis exacerbates the pathological response and promotes collagen production by cardiac fibroblasts to exacerbate myocardial fibrosis (40). This finding was previously confirmed by the limited development of autoimmune myocarditis in IL-6 knockout mice (41). IL-1β is a potent proinflammatory cytokine that activates T cells and induces cytokine production (39). TAB1 is a protein activator of TAK1. The TAB1-TAK1 complex is involved in NF-κB activation (32,42). Overexpression of IL-1β, TNF-α and IL-6 can all activate NF-κB through the TAB1 pathway (43). This activated NF-κB then translocates to the nucleus as a transcription factor to activate the expression of inflammatory cytokines (44). This process leads to a cascade amplification response mediated among inflammatory cytokines to sustain chronic cardiomyocyte necrosis and infiltration of inflammatory cells (45). It is the activation of this vicious cycle that exacerbates myocardial injury (45). Therefore, TAB1 serves a key role in the regulation of the immune-inflammatory response. Importantly, inhibition of TAB1/NF-κB signaling and secretion of TNF-α, IL-6 and IL-1β can effectively prevent myocardial inflammation and remodeling (46-49).

The present study showed that treatment of EAM mice with KX ameliorated myocardial injury in a dose-dependent manner, in addition to inhibiting the secretion of TNF-α, IL-6, IL-1β and NF-κB signaling proteins. Therefore, KX may reduce inflammation through the TAB1/NF-κB pathway to reduce myocardial injury. Numerous modern pharmacological studies have previously shown that the *Sophora flavescens* family of TCM can reduce the levels of TNF-α and IL-1β in ethanol-induced acute gastric ulcer rat model and lipopolysaccharide-induced inflammation in zebrafish through the NF-κB signaling pathway (18,50,51). Combined with the findings of the present study, it was therefore hypothesized that *Sophora flavescens* alkaloids in KX may serve a therapeutic role in the first stage of EAM by inhibiting inflammatory responses. Nevertheless, further investigation is warranted to validate this finding.

TGF-β1 is an anti-inflammatory cytokine secreted by macrophages that are activated by regulatory T-cells (52). Members of the TGF-β family bind to type II receptors and recruit type I receptors, leading to the phosphorylation and activation of type I receptors (53). In turn, type I receptors phosphorylate the Smad downstream effector molecules, including Smad1, Smad2, Smad3, Smad5 and Smad8, which translocate to the nucleus to promote the expression of fibrotic genes, such as effector connective tissue growth factor (CTGF), Col I and Col III (54). TGF-β1 can also convert fibroblasts into myofibroblasts, which synthesize and secrete fibrillar Col I and Col III to promote the development of myocardial fibrosis (55). Previous studies have shown that inhibition of TGF-β1 can reduce the production of Col I and Col III to prevent myocardial fibrosis (56,57). Hao *et al* (58) reported that the mRNA expression and promotion of Col I synthesis by TGF-β1 was eliminated by blocking Smad expression in the myocardial infarct rat model, suggesting that TGF-β1 and Smad are involved in collagen synthesis. Therefore, inhibition of the TGF-β1 pathway may be key to the treatment of myocardial fibrosis (12). In the present study, the levels of TGF-β1, Col I and Col III, in addition to the degree of myocardial fibrosis, were all significantly reduced in EAM mice treated with KX after 60 days in a dose-dependent manner. This treatment also significantly reduced the expression of TGF-β1/Smad2 pathway signaling components in the myocardial tissue. It is suggested that KX may delay the development of myocardial fibrosis and irreversible pathological changes to the myocardium through the TGF-β1/Smad2 pathway in mice with inflammatory myocardial injury. A number of pharmacological studies have shown that treatment with American ginseng (*Panax quinquefolium*) can delay myocardial fibrosis and cardiac remodeling in animal models through the TGF-β1/Smad signaling pathway (17,19-21). Collectively, the previous and present results indicate that *Panax quinquefolium* saponins contained in KX can exert a therapeutic effect on the second stage of EAM by delaying the development of myocardial fibrosis.

Based on the present findings, KX may be efficacious for the clinical treatment of myocarditis by attenuating the inflammatory response whilst alleviating the clinical symptoms in acute myocarditis. KX may be effective in delaying progression even in patients in which the treatment of myocarditis is delayed. This provides an important reference value for the clinical application of KX.

However, the present study remain associated with a number of limitations. There was lack of a positive control group. *Astragalus membranaceus* would be the ideal positive control group for this study. However, the present study was rather focused on the effects of KX on different stages of autoimmune myocarditis and made comparisons among different stages. The present study also did not measure oxidative stress parameters, which can provide evidence of cell damage. There was a lack of echocardiography test results, which are critical for cardiac function assessment in mice. Analysis of cardiac function by echocardiography, along with the effect of KX on the differentiation of $CD4^+$ T cells, would be of potential interest for future studies.

Results of the present study suggested that KX may reduce the inflammatory response to autoimmune myocarditis and attenuate pathological injury during the first stage of EAM through the TAB1/NF-κB pathway. Subsequently, KX may

also delay the progression of autoimmune myocarditis onto myocardial fibrosis through the TGF-β1/Smad2 pathway during the second stage of EAM. This reflects the multi-faceted, multi-target and multi-pathway action of KX in the treatment of myocarditis, in addition to the synergy among Chinese herbal therapies. However, in the present study, there is insufficient evidence to state that *Sophora flavescens* alkaloids and *Panax quinquefolium* saponins inhibit the first and second phases of EAM, respectively.

Acknowledgements

Not applicable.

Funding

The present study was supported by the Jilin Science and Technology Development Plan Project (grant no. 20200403128SF).

Availability of data and materials

The datasets used and/or analyzed during the current study are available from the corresponding author on reasonable request.

Authors' contributions

LL and TD made substantial contributions to the conception and design of the study. ML and YL were responsible for the experimental procedures, data acquisition, analysis and interpretation and confirm the authenticity of all the raw data. ML performed the drafting of the article and critically revised it for important intellectual content. HX was responsible for the review of data and experiments. All authors read and approved the final manuscript. All authors agree to be accountable for all aspects of the work in ensuring that questions related to the accuracy or integrity of the work are appropriately investigated and resolved.

Ethics approval and consent to participate

All experiments and animal care procedures were approved by the animal ethics committee of Jilin Academy of Traditional Chinese Medicine(approval no. JLSZKYDWLL2021-003).

Patient consent for publication

Not applicable.

Competing interests

The authors declare that they have no competing interests.

References

1. Tschöpe C, Ammirati E, Bozkurt B, Caforio ALP, Cooper LT, Felix SB, Hare JM, Heidecker B, Heymans S, Hübner N, *et al*: Myocarditis and inflammatory cardiomyopathy: Current evidence and future directions. Nat Rev Cardiol 18: 169-193, 2021.
2. Canter CE and Simpson KE: Diagnosis and treatment of myocarditis in children in the current era. Circulation 129: 115-128, 2014.
3. Jaén RI, Fernández-Velasco M, Terrón V, Sánchez-García S, Zaragoza C, Canales-Bueno N, Val-Blasco A, Vallejo-Cremades MT, Boscá L and Prieto P: BML-111 treatment prevents cardiac apoptosis and oxidative stress in a mouse model of autoimmune myocarditis. FASEB J 34: 10531-10546, 2020.
4. Fairweather D, Kaya Z, Shellam GR, Lawson CM and Rose NR: From infection to autoimmunity. J Autoimmun 16: 175-186, 2001.
5. Błyszczuk P: Myocarditis in humans and in experimental animal models. Front Cardiovasc Med 6: 64, 2019.
6. Cihákova D, Sharma RB, Fairweather D, Afanasyeva M and Rose NR: Animal models for autoimmune myocarditis and autoimmune thyroiditis. Methods Mol Med 102: 175-193, 2004.
7. Pollack A, Kontorovich AR, Fuster V and Dec GW: Viral myocarditis-diagnosis, treatment options, and current controversies. Nat Rev Cardiol 12: 670-680, 2015.
8. Neu N, Rose NR, Beisel KW, Herskowitz A, Gurri-Glass G and Craig SW: Cardiac myosin induces myocarditis in genetically predisposed mice. J Immunol 139: 3630-3636, 1987.
9. Blyszczuk P, Behnke S, Lüscher TF, Eriksson U and Kania G: GM-CSF promotes inflammatory dendritic cell formation but does not contribute to disease progression in experimental autoimmune myocarditis. Biochim Biophys Acta 1833: 934-944, 2013.
10. van Heeswijk RB, De Blois J, Kania G, Gonzales C, Blyszczuk P, Stuber M, Eriksson U and Schwitter J: Selective in vivo visualization of immune-cell infiltration in a mouse model of autoimmune myocarditis by fluorine-19 cardiac magnetic resonance. Circ Cardiovasc Imaging 6: 277-284, 2013.
11. Li Y, Heuser JS, Cunningham LC, Kosanke SD and Cunningham MW: Mimicry and antibody-mediated cell signaling in autoimmune myocarditis. J Immunol 177: 8234-8240, 2006.
12. Blyszczuk P, Müller-Edenborn B, Valenta T, Osto E, Stellato M, Behnke S, Glatz K, Basler K, Lüscher TF, Distler O, *et al*: Transforming growth factor-β-dependent Wnt secretion controls myofibroblast formation and myocardial fibrosis progression in experimental autoimmune myocarditis. Eur Heart J 38: 1413-1425, 2017.
13. Tajiri K, Imanaka-Yoshida K, Tsujimura Y, Matsuo K, Hiroe M, Aonuma K, Ieda M and Yasutomi Y: A new mouse model of chronic myocarditis induced by recombinant bacille calmette-guèrin expressing a t-cell epitope of cardiac myosin heavy chain-α. Int J Mol Sci 22: 794, 2021.
14. Kleinert S, Weintraub RG, Wilkinson JL and Chow CW: Myocarditis in children with dilated cardiomyopathy: Incidence and outcome after dual therapy immunosuppression. J Heart Lung Transplant 16: 1248-1254, 1997.
15. Felix SB, Staudt A, Dörffel WV, Stangl V, Merkel K, Pohl M, Döcke WD, Morgera S, Neumayer HH, Wernecke KD, *et al*: Hemodynamic effects of immunoadsorption and subsequent immunoglobulin substitution in dilated cardiomyopathy: Three-month results from a randomized study. J Am Coll Cardiol 35: 1590-1598, 2000.
16. De Luca G, Campochiaro C, Sartorelli S, Peretto G, Sala S, Palmisano A, Esposito A, Candela C, Basso C, Rizzo S, *et al*: Efficacy and safety of mycophenolate mofetil in patients with virus-negative lymphocytic myocarditis: A prospective cohort study. J Autoimmun 106: 102330, 2020.
17. Zhang YJ, Zhang XL, Li MH, Iqbal J, Bourantas CV, Li JJ, Su XY, Muramatsu T, Tian NL and Chen SL: The ginsenoside Rg1 prevents transverse aortic constriction-induced left ventricular hypertrophy and cardiac dysfunction by inhibiting fibrosis and enhancing angiogenesis. J Cardiovasc Pharmacol 62: 50-57, 2013.
18. Niu Y, Dong Q and Li R: Matrine regulates Th1/Th2 cytokine responses in rheumatoid arthritis by attenuating the NF-κB signaling. Cell Biol Int 41: 611-621, 2017.
19. Zheng X, Wang S, Zou X, Jing Y, Yang R, Li S and Wang F: Ginsenoside Rb1 improves cardiac function and remodeling in heart failure. Exp Anim 66: 217-228, 2017.
20. Wang QW, Yu XF, Xu HL, Zhao XZ and Sui DY: Ginsenoside re improves isoproterenol-induced myocardial fibrosis and heart failure in rats. Evid Based Complement Alternat Med 2019: 3714508, 2019.
21. Li CY, Deng W, Liao XQ, Deng J, Zhang YK and Wang DX: The effects and mechanism of ginsenoside Rg1 on myocardial remodeling in an animal model of chronic thromboembolic pulmonary hypertension. Eur J Med Res 18: 16, 2013.
22. Yin HJ, Zhang Y and Jiang YR: Effect of folium panax quinquefolium saponins on apoptosis of cardiac muscle cells and apoptosis-related gene expression in rats with acute myocardial infarction. Zhongguo Zhong Xi Yi Jie He Za Zhi 25: 232-235, 2005 (In Chinese).

23. Wei N, Zhang C, He H, Wang T, Liu Z, Liu G, Sun Z, Zhou Z, Bai C and Yuan D: Protective effect of saponins extract from Panax japonicus on myocardial infarction: Involvement of NF-κB, Sirt1 and mitogen-activated protein kinase signalling pathways and inhibition of inflammation. J Pharm Pharmacol 66: 1641-1651, 2014.
24. Szczuka D, Nowak A, Zakłos-Szyda M, Kochan E, Szymańska G, Motyl I and Blasiak J: American ginseng (Panax quinquefolium L.) as a source of bioactive phytochemicals with pro-health properties. Nutrients 11: 1041, 2019.
25. He X, Fang J, Huang L, Wang J and Huang X: *Sophora flavescens* Ait: Traditional usage, phytochemistry and pharmacology of an important traditional Chinese medicine. J Ethnopharmacol 172: 10-29, 2015.
26. Zhang G, Tang Y, Shang J, Wang Z, Yu H, Du W and Fu Q: Flow-injection chemiluminescence method to detect a β2 adrenergic agonist. Luminescence 30: 102-109, 2015.
27. Ding T, Liu B, Wang X, Wen FC, Ji FL, Song LL and Xu HB: Effects of KX composition and single ingredient on the model of autoimmunity myocarditis. Chi J Tradit Chin Med Pharm 32: 3710-3712, 2017 (In Chinese).
28. Aretz HT: Myocarditis: The dallas criteria. Hum Pathol 18: 619-624, 1987.
29. Sinagra G, Anzini M, Pereira NL, Bussani R, Finocchiaro G, Bartunek J and Merlo M: Myocarditis in clinical practice. Mayo Clin Proc 91: 1256-1266, 2016.
30. Li Y, Yu P, Fu W, Cai L, Yu Y, Feng Z, Wang Y, Zhang F, Yu X, Xu H and Sui D: Ginseng-Astragalus-oxymatrine injection ameliorates cyclophosphamide-induced immunosuppression in mice and enhances the immune activity of RAW264.7 cells. J Ethnopharmacol 279: 114387, 2021.
31. Zhang S, Liu X, Sun C, Yang J, Wang L, Liu J, Gong L and Jing Y: Apigenin attenuates experimental autoimmune myocarditis by modulating Th1/Th2 cytokine balance in mice. Inflammation 39: 678-686, 2016.
32. Sagar S, Liu PP and Cooper LT Jr: Myocarditis. Lancet 379: 738-747, 2012.
33. Wang J, Liu T, Chen X, Jin Q, Chen Y, Zhang L, Han Z, Chen D, Li Y, Lv Q and Xie M: Bazedoxifene regulates Th17 immune response to ameliorate experimental autoimmune myocarditis via inhibition of STAT3 activation. Front Pharmacol 11: 613160, 2020.
34. Muller AM, Fischer A, Katus HA and Kaya Z: Mouse models of autoimmune diseases-autoimmune myocarditis. Curr Pharm Des 21: 2498-2512, 2015.
35. Li J, Schwimmbeck PL, Tschope C, Leschka S, Husmann L, Rutschow S, Reichenbach F, Noutsias M, Kobalz U, Poller W, *et al*: Collagen degradation in a murine myocarditis model: Relevance of matrix metalloproteinase in association with inflammatory induction. Cardiovascular Res 56: 235-247, 2002.
36. Izumi T, Takehana H, Matsuda C, Yokoyama H, Kohno K, Suzuki K and Inomata T: Experimental autoimmune myocarditis and its pathomechanism. Herz 25: 274-278, 2000.
37. Esfandiarei M and McManus BM: Molecular biology and pathogenesis of viral myocarditis. Annu Rev Pathol 3: 127-155, 2008.
38. Liu T, Yang F, Liu J, Zhang M, Sun J, Xiao Y, Xiao Z, Niu H, Ma R, Wang Y, *et al*: Astragaloside IV reduces cardiomyocyte apoptosis in a murine model of coxsackievirus B3-induced viral myocarditis. Exp Anim 68: 549-558, 2019.
39. Camporeale A and Poli V: IL-6, IL-17 and STAT3: A holy trinity in auto-immunity? Front Biosci (Landmark Ed) 17: 2306-2326, 2012.
40. Meléndez GC, McLarty JL, Levick SP, Du Y, Janicki JS and Brower GL: Interleukin 6 mediates myocardial fibrosis, concentric hypertrophy, and diastolic dysfunction in rats. Hypertension 56: 225-231, 2010.
41. Eriksson U, Kurrer MO, Schmitz N, Marsch SC, Fontana A, Eugster HP and Kopf M: Interleukin-6-deficient mice resist development of autoimmune myocarditis associated with impaired upregulation of complement C3. Circulation 107: 320-325, 2003.
42. Shim JH, Xiao C, Paschal AE, Bailey ST, Rao P, Hayden MS, Lee KY, Bussey C, Steckel M, Tanaka N, *et al*: TAK1, but not TAB1 or TAB2, plays an essential role in multiple signaling pathways in vivo. Genes Dev 19: 2668-2681, 2005.
43. Yang C, Yang C, Zhang J, Guo Y, Chen N, Yin B, Zhou Q, Zhang T, Guo S and Deng G: MicroRNA-211 regulates the expression of TAB1 and inhibits the NF-κB signaling pathway in lipopolysaccharide-induced endometritis. Int Immunopharmacol 96: 107668, 2021.
44. Cheng Z, Taylor B, Ourthiague DR and Hoffmann A: Distinct single-cell signaling characteristics are conferred by the MyD88 and TRIF pathways during TLR4 activation. Sci Signal 8: ra69, 2015.
45. Libby P, Nahrendorf M and Swirski FK: Leukocytes link local and systemic inflammation in ischemic cardiovascular disease: An expanded 'Cardiovascular Continuum'. J Am Coll Cardiol 67: 1091-1103, 2016.
46. Liu T, Zhang M, Niu H, Liu J, Ruilian M, Wang Y, Xiao Y, Xiao Z, Sun J, Dong Y and Liu X: Astragalus polysaccharide from astragalus melittin ameliorates inflammation via suppressing the activation of TLR-4/NF-κB p65 signal pathway and protects mice from CVB3-induced virus myocarditis. Int J Biol Macromol 126: 179-186, 2019.
47. Xue YL, Zhang SX, Zheng CF, Li YF, Zhang LH, Hao YF, Wang S and Li XW: Silencing of STAT4 protects against autoimmune myocarditis by regulating Th1/Th2 immune response via inactivation of the NF-κB pathway in rats. Inflammation 42: 1179-1189, 2019.
48. Pan A, Tan Y, Wang Z and Xu G: STAT4 silencing underlies a novel inhibitory role of microRNA-141-3p in inflammation response of mice with experimental autoimmune myocarditis. Am J Physiol Heart Circ Physiol 317: H531-H540, 2019.
49. Zhu Z, Xueying L, Chunlin L, Wen X, Rongrong Z, Jing H, Meilan J, Yuwei X and Zili W: Effect of berberine on LPS-induced expression of NF-κB/MAPK signalling pathway and related inflammatory cytokines in porcine intestinal epithelial cells. Innate Immun 26: 627-634, 2020.
50. Hu J, Luo J, Zhang M, Wu J, Zhang Y, Kong H, Qu H, Cheng G and Zhao Y: Protective effects of radix sophorae flavescentis carbonisata-based carbon dots against ethanol-induced acute gastric ulcer in rats: Anti-Inflammatory and antioxidant activities. Int J Nanomedicine 16: 2461-2475, 2021.
51. Hwang SJ, Song YS and Lee HJ: Phaseolin attenuates lipopolysaccharide-induced inflammation in RAW 264.7 cells and zebrafish. Biomedicines 9: 420, 2021.
52. Noack M and Miossec P: Th17 and regulatory T cell balance in autoimmune and inflammatory diseases. Autoimmun Rev 13: 668-677, 2014.
53. Morikawa M, Derynck R and Miyazono K: TGF-β and the TGF-β Family: Context-dependent roles in cell and tissue physiology. Cold Spring Harb Perspect Biol 8: a021873, 2016.
54. Biernacka A, Dobaczewski M and Frangogiannis NG: TGF-β signaling in fibrosis. Growth Factors 29: 196-202, 2011.
55. Cowling RT, Kupsky D, Kahn AM, Daniels LB and Greenberg BH: Mechanisms of cardiac collagen deposition in experimental models and human disease. Transl Res 209: 138-155, 2019.
56. Zhang Y, Wang J, Li H, Yuan L, Wang L, Wu B and Ge J: Hydrogen sulfide suppresses transforming growth factor-β1-induced differentiation of human cardiac fibroblasts into myofibroblasts. Sci China Life Sci 58: 1126-1134, 2015.
57. Johnston EF and Gillis TE: Transforming growth factor beta-1 (TGF-β1) stimulates collagen synthesis in cultured rainbow trout cardiac fibroblasts. J Exp Biol 220: 2645-2653, 2017.
58. Hao J, Ju H, Zhao S, Junaid A, Scammell-La Fleur T and Dixon IM: Elevation of expression of Smads 2, 3, and 4, decorin and TGF-beta in the chronic phase of myocardial infarct scar healing. J Mol Cell Cardiol 31: 667-678, 1999.